TISSUE-SPECIFIC STEM CELLS

Prospective Isolation of Skeletal Muscle Stem Cells with a Pax7 Reporter

DARKO BOSNAKOVSKI,[a] ZHAOHUI XU,[b] WEI LI,[b] SUWANNEE THET,[b] ONDINE CLEAVER,[c] RITA C.R. PERLINGEIRO,[a] MICHAEL KYBA[a]

[a]Lillehei Heart Institute and Department of Pediatrics, University of Minnesota, Minneapolis, Minnesota, USA; Departments of [b]Developmental Biology and [c]Molecular Biology, University of Texas Southwestern Medical Center, Dallas, Texas, USA

ABSTRACT

Muscle regeneration occurs through activation of quiescent satellite cells whose progeny proliferate, differentiate, and fuse to make new myofibers. We used a transgenic Pax7-ZsGreen reporter mouse to prospectively isolate stem cells of skeletal muscle by flow cytometry. We show that Pax7-expressing cells (satellite cells) in the limb, head, and diaphragm muscles are homogeneous in size and granularity and uniformly labeled by certain cell surface markers, including CD34 and CD29. The frequency of the satellite cells varies between muscle types and with age. Clonal analysis demonstrated that all colonies arising from single cells within the Pax7-sorted fraction have myogenic potential. In response to injury, Pax7$^+$ cells reduce CD34, CD29, and CXCR4 expression, increase in size, and acquire Sca-1. When directly isolated and cultured in vitro, Pax7$^+$ cells display the hallmarks of activation and proliferate, initially as suspension aggregates and later distributed between suspension and adherence. During in vitro expansion, Pax7 (ZsGreen) and CD34 expression decline, whereas expression of PSA-NCAM is acquired. The nonmyogenic, Pax7^{neg} cells expand as Sca1$^+$ PDGRα^+ PSA-NCAM^{neg} cells. Satellite cells expanded exclusively in suspension can engraft and produce dystrophin$^+$ fibers in mdx$^{-/-}$ mice. These results establish a novel animal model for the study of muscle stem cell physiology and a culture system for expansion of engraftable muscle progenitors. STEM CELLS 2008;26:3194–3204

Disclosure of potential conflicts of interest is found at the end of this article.

INTRODUCTION

Skeletal muscle is composed of highly specialized and terminally differentiated multinuclear, postmitotic myofibers. Growth, maintenance, and regeneration of skeletal muscle therefore depends on an undifferentiated mononuclear muscle progenitor pool, of which satellite cells are the principal component [1, 2]. Satellite cells are mitotically quiescent mononuclear cells located beneath the basal lamina of each muscle fiber, with the ability to undergo proliferation and myogenic differentiation [3, 4]. Morphologically, they are characterized by a high nucleus-to-cytoplasm ratio and a reduced organelle content [5]. The capacity for lifelong muscle regeneration through generation of new pools of myoblasts is supported by a tremendous capacity of satellite cells for self-renewal [6, 7].

Much evidence suggests that the satellite cell pool is heterogeneous [8]. Various surface markers, including CD34 [9], CXCR4 and CD29 [10, 11], syndecan 3 and 4 [12], M-cadherin [13], and c-met [14], have been detected on at least some fraction of satellite cells [9, 15]. This variety is compounded by functional differences observed upon in vitro clonal analysis. Single satellite cells give rive to clones with various proliferative abilities and myogenic potentials, and some clones even spontaneously give rise to cells with fibroblastic and adipogenic character [9, 10, 16, 17]. In spite of this variability, there is consensus that the expression of Pax7 in adult mice marks the satellite cells with myogenic stem cell potential [18]. Pax7 is a paired-box transcription factor that shares significant redundancy with its homolog Pax3 [19] in the development of skeletal muscle and dorsal neural tube (reviewed in [20]). The majority of neonatal satellite cells descend from the same somite-derived Pax3$^+$/Pax7$^+$ population that gives rise to the embryonic musculature [21, 22]. In adult muscle, Pax7 is expressed in quiescent and activated satellite cells, as well as in proliferating myogenic progenitors, and is downregulated prior to myoblast differentiation and fusion [23]. Muscle stem cell activity in the Pax7 null mouse is ablated, and the few Pax7^{neg} cells located in the sublaminar satellite position of this mouse arrest and die upon entering mitosis [23].

It has been reported recently that Pax7-expressing satellite cells are functionally heterogeneous based on Myf5 expression history. Transplantation experiments reveal that Pax7$^+$ satellite cells that express or have expressed Myf5 are able to contribute to myofiber formation but reconstitute the satellite cell compartment poorly, whereas satellite cells that have never expressed Myf5 contribute to the satellite cell reservoir efficiently and give rise to Pax7$^+$/Myf5$^+$ cells, which further contribute to myofiber formation [8].

Contradictory reports about satellite cell phenotype and character are most likely due to differences in methodology for isolation and to technical factors, including specificity of antibodies. Various nonsatellite cell types associated with the muscle have also been ascribed myogenic activity. Among these are Pax3-expressing cells, located in the interstitial space of the skeletal muscle [24]; side population cells [25]; muscle-resident CD45^{+} cells [26]; and perivascular cells from human skeletal muscle [27].

Considering the exclusive expression of Pax7 in satellite cells and the importance of this gene in the regulation of muscle regeneration, we generated a Pax7-ZsGreen mouse reporter strain. These mice allow direct access to the satellite cell pool by flow cytometry, enabling both a precise in vivo characterization and the direct isolation of a homogeneous cell population for in vitro study.

MATERIALS AND METHODS

Antibodies

We used the following primary antibodies: monoclonal mouse anti-MyoD (1:250), anti-M-cadherin (1:100), rat anti-mouse CD105 (1:100), rat anti-mouse platelet-derived growth factor receptor α (PDGFRα) (1:100), rat anti-mouse CD29 (1:100; integrin $\beta 1$ chain), biotin-conjugated anti-mouse CXCR4 (1:100; CD184), APC-conjugated goat-anti-mouse, APC-conjugated goat-anti-rat and APC-conjugated streptavidin, all from BD Biosciences (San Diego, http://www.bdbiosciences.com); biotin-conjugated anti-mouse CD34 (1:100; clone RAM34) and Sca1 (1:100; Ly-6A/E; clone D7); APC-conjugated Flk-1 (1:100; clone avas12a1) and APC-conjugated c-Kit (1:100), all from eBioscience Inc. (San Diego, http://www.ebioscience.com); monoclonal anti-mouse PSA-NCAM (1:500) and anti-M-cadherin (1:50) from Calbiochem (San Diego, http://www.emdbiosciences.com); and monoclonal mouse anti-Pax7 and myosin heavy chain (MyHC; 1:10; Developmental Studies Hybridoma Bank, Iowa City, IA, http://www.uiowa.edu/ ~dshbwww, developed under the auspices of the NICHD and maintained by the University of Iowa).

Generation of Pax7-ZsGreen Mice

The Pax7 BAC (RP23–218H13) was modified by recombineering in *Escherichia coli* to introduce ZsGreen into the first coding exon, replacing the Pax7 coding sequence. Recombination arms were amplified from the BAC using the following primers (restriction sites are underlined): upF, CTCGAGCCTTCCCTGCCGTTGA; upR, GTCGACGCACGCTGGAGACGAAT; downF, AGATCTC-CCCAGGATGATGAGACC; downR, CGGCCGGGGAGGAAGC-GGACGGT. They were then cloned into pL451-FX (a version of pL451 in which one FseI site was destroyed to be able to excise the replacement sequence as an FseI/XhoI fragment) as an XhoI/SalI fragment into the XhoI site (upstream) and BglII/EagI fragment into BamHI and NotI (downstream) sites. ZsGreen was then inserted as an XhoI/NotI (blunted) fragment into SalI/EcoRV sites. *E. coli* EL250 carrying the Pax7 BAC were temperature-shifted and transformed with the replacement sequence (excised using FseI and XhoI digestion), and the recombinant was selected with neomycin as described [28]. The *neo* gene was subsequently removed by inducing Flp recombinase with arabinose, and the recombinant BAC was purified and used for pronuclear injection.

Fluorescence-Activated Cell Sorting of Pax7-ZsGreen[+] Cells

Muscles from Pax7-ZsGreen mice were aseptically dissected, ground to small pieces, and digested with collagenase type I (Invitrogen, Carlsbad, CA, http://www.invitrogen.com) for 75 minutes at 37°C. Pellets of the muscle digest were extensively washed by phosphate-buffered saline (PBS), and a single-cell suspension was obtained after filtering the samples through 70-μm cell strainers

(BD Biosciences). For live cell sorting, single-cell suspension was pelleted and resuspended in PBS containing 2% fetal bovine serum (FBS) and 1 μg/ml propidium iodide (PI) to identify and exclude dead (PI^{+}) cells. For antibody staining, cells were suspended in PBS/2% FBS and incubated with primary antibody for 30 minutes, and when necessary with secondary antibody for 20 minutes on ice. Cells were washed twice with PBS/2% FBS, flow cytometric sorting and analyses were performed on a FACSAria (BD Biosciences), and data were analyzed using FlowJo (BD Biosciences).

Cell Culture

Cells were cultured in proliferation medium comprising a 1:1 mixture of high-glucose Dulbecco's modified Eagle's medium (DMEM) and Ham's F-12 Nutrient Mixture (Gibco, Grand Island, NY, http://www.invitrogen.com), supplemented with 1% chick embryonic extract; 10 ng/ml basic fibroblast growth factor (bFGF; Peprotech, Rocky Hill, NJ, http://www.peprotech.com); 20% FBS (Atlanta Biologicals, Lawrenceville, GA, http://www.atlantabio. com); 10% horse serum (HS; Sigma-Aldrich, St. Louis, http://www. sigmaaldrich.com); penicillin, streptomycin, and gentamicin (Gibco); and 0.25 μg/ml amphotericin B (Sigma-Aldrich), at 37°C in 5% O_2/5% CO_2. For myogenic differentiation, cells were cultured on gelatin-coated dishes in proliferation medium until they reached confluence and then washed with serum-free DMEM and differentiated with DMEM supplemented with 2% HS and insulin (Sigma-Aldrich) for 2–4 days. The C2C12 cell line was cultured in DMEM (high-glucose) supplemented with 20% FBS and penicillin/ streptomycin. Live cell images were captured on an Olympus IX70 microscope (Olympus, Tokyo, http://www.olympus-global.com) with a Nikon DXM1200 digital camera (Nikon, Tokyo, http://www. nikon.com) and Nikon ACT-1 software.

Muscle Injury Cell Transplantation

For analyses of activated satellite cells, left hind limbs of Pax7-ZsGreen mice were injured with 500 μl in multiple injections of 1 μM cardiotoxin (*Naja nigricollis*; Calbiochem), and 3 days postinjury, analysis was performed. For transplantation, dystrophin-deficient mice (mdx^{−/−}; Jackson Laboratory, Bar Harbor, ME, http:// www.jax.org) immunosuppressed with 500 μg/ml tacrolimus (ChemPacific, Baltimore, http://www.chempacific.com) were used. Tibialis anterior (TA) muscles of mdx^{−/−} mice were injured by 100 μl of cardiotoxin 24 hours before transplantation. Pax7-ZsGreen^{+} cells expanded for 8 days in culture were resuspended in PBS (2,000 or 10,000 cells in 10 μl of PBS) and injected into injured TA muscle [6]. Three weeks after transplantation TA muscles were harvested and quick-frozen in Tissue-Tek OCT Compound (Sakura Finetek, Torrance, CA, http://www.sakura.com) compound and stored at −80°C. Analyses and quantification of the dystrophin-positive fibers were done as described previously [6] by counting the dystrophin-positive muscle fibers in representative transverse sections from the mid-belly (n = 4) of the TA muscle.

Immunofluorescence

Cells cultured on gelatin-coated chamber slides or 8-μm tissue cryosections were fixed with 4% paraformaldehyde for 20 minutes, permeabilized by 0.3% Triton X-100 for 30 minutes, and blocked with 10% goat serum for 1 hour at room temperature. Slides were exposed to primary antibodies in PBS/2% goat serum at 4°C overnight or at room temperature for 60 minutes, followed by secondary Cy3- or Cy2-conjugated antibodies (1:400; Sigma-Aldrich) at room temperature for 45 minutes. Cells were counterstained with 4′,6-diamidino-2-phenylindole (Invitrogen) to visualize nuclei and mounted in Immu-Mount (Thermo Scientific Inc., Pittsburgh, http:// www.thermo.com). The images were visualized with an Olympus BX50 microscope, an Olympus U-CMAD digital camera, and MetaVue 5.0 software (Molecular Devices Corp., Union City, CA, http://www.moleculardevices.com).

Quantitative Real-Time Reverse Transcription-Polymerase Chain Reaction

Total RNA was extracted with Trizol (Invitrogen), and cDNA was generated using 1 μg of DNase-treated RNA with oligo(dT) primer
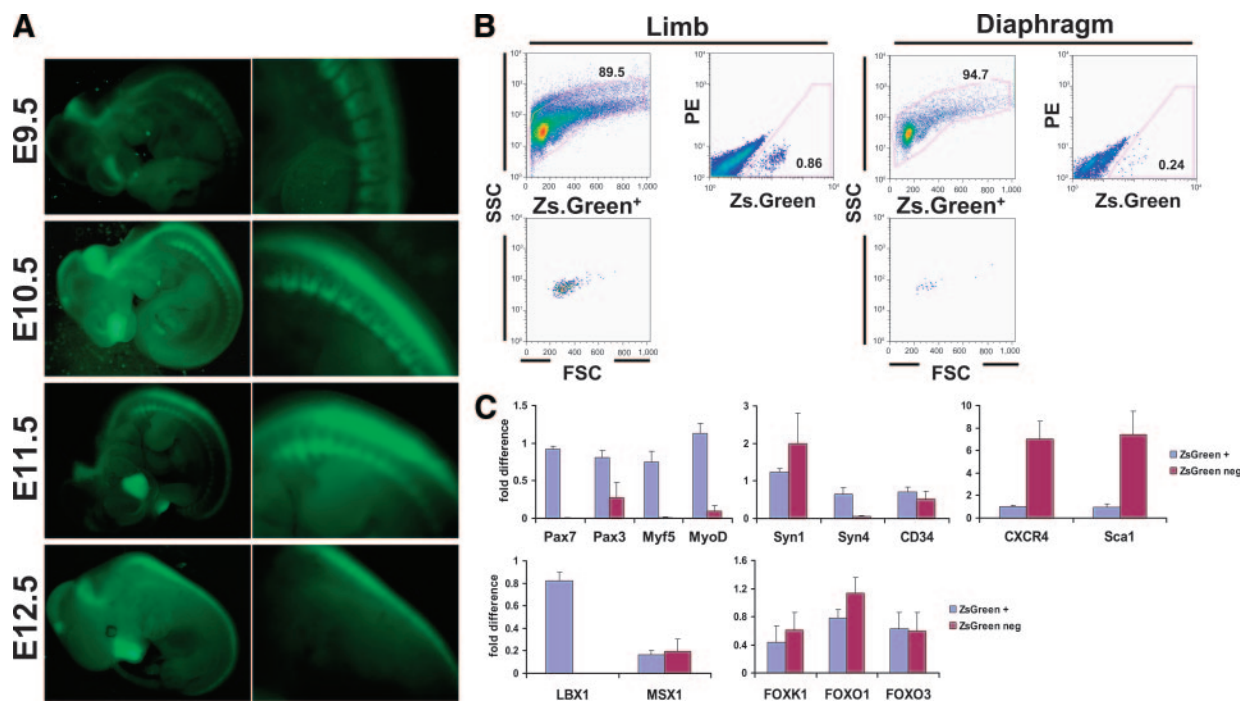
Figure 1. ZsGreen fluorescence recapitulates Pax7 expression. **(A):** ZsGreen expression in embryos from E9.5 to E12.5. Note that green florescence is exclusively localized in the somite, frontonasal processes, and the neural tube. **(B):** Fluorescence-activated cell sorting profile of muscle digests from Pax7-ZsGreen mice. The upper left panel shows the FSC/SSC profile of total cells. The upper right panel shows fluorescence of live cells (gated using propidium iodide, not shown) in the FSC/SSC gate indicated at the left. Green fluorescence is shown on the x-axis, and red fluorescence is shown on the y-axis. This uncompensated two-dimensional representation allows maximum separation of autofluorescent cells, which track along the diagonal, from the weak true green fluorescent population, which is shifted to the right of the diagonal. The lower panel shows the FSC/SSC profile of total live cells in the ZsGreen gate indicated. Note that green cells were homogeneous in size (FSC) and granularity (SSC). **(C):** Real-time reverse transcription-polymerase chain reaction on ZsGreen⁺ or -neg cells directly sorted from hind limb muscle of 3-month-old male mice. Results are presented as fold difference comparing ZsGreen-positive with -neg cells; data represent mean $\pm$ SE ($n = 3$). Abbreviations: E, embryonic day; FSC, forward scatter; neg, negative; SSC, side scatter.

and ThermoScript (Invitrogen). Polymerase chain reaction (PCR) was performed by using TaqMan Real-Time PCR premixture on a 7500 Real-Time PCR System (Applied Biosystems, Foster City, CA, http://www.appliedbiosystems.com). Premade primer and probe sets were purchased from Applied Biosystems. Data were normalized to glyceraldehyde-3-phosphate dehydrogenase and analyzed by 7500 System software (Applied Biosystems).

RESULTS

Generation of a Pax7-ZsGreen Reporter Mouse

We modified a murine BAC containing the Pax7 locus by replacing the Pax7 coding sequence from exon 1 with a sequence encoding ZsGreen, and we generated transgenic mice by pronuclear injection. To confirm whether green fluorescence recapitulated expression of Pax7, we analyzed the ZsGreen expression pattern during embryonic development. Clearly detectible green signal was observed in the somites, frontonasal processes, and the neural tube, as early as 9.5 days of gestation (Fig. 1A). The intensity of the signal increased at embryonic day 10.5 and following, and the signal remained localized to the defined Pax7-expressing areas [19]. To further validate specificity, we evaluated expression in various adult tissues. Skeletal muscle, heart, lung, spleen, liver, intestine, bladder, uterus, and kidney were enzymatically digested to single-cell suspensions and analyzed by flow cytometry. Fluorescent cells were detected only in skeletal muscle (data not shown), and they were homogeneous in size and granularity (Fig. 1B). At 1 month of age, the frequency of positive cells within the mononuclear cell fraction

from total hind limb muscles digests averaged 0.8%. Pax7-ZsGreen⁺ cells from the diaphragm displayed the same small size and low granularity as those from the hind limb and were present at half the frequency (Fig. 1B). To further confirm that ZsGreen expression mirrored that of Pax7, we sorted 10,000 positive and negative cells from 3-month-old male mice ($n = 3$) and investigated Pax7 expression by reverse transcription (RT)-PCR. We found expression of Pax7 only in the ZsGreen⁺ fraction (Fig. 1C). Analyses of other myogenic transcripts, satellite cell markers, and genes characteristic of quiescent cells showed that green cells expressed significantly more Myf5, MyoD, Syn4, and Lbx1 compared with the negative cells (Fig. 1C). The expression levels of CD34, Syn1, Msx1, Foxk1, Foxo1, and Foxo3 in the positive cells were comparable to those in the negative cells. Many of these markers are expected to be expressed by nonmuscle cells (e.g., CD34 by endothelial cells, Foxo factors by various quiescent cells). Finally, significant overexpression of Sca1 and CXCR4 was detected in negative cells. These results correlate with the fluorescence-activated cell sorting analyses, which showed that a high percentage of Pax7ⁿᵉᵍ mononuclear cells were labeled with CD34, CXCR4, and Sca1 (Figs. 1C, 3). In addition, basal (very low) expression of Pax3 was detected in both negative and positive fractions. (Fig. 1C) [24, 29, 30]. We evaluated muscle sections but were not able to detect ZsGreen by immunohistochemistry, a result that we attribute in part to the quality of the available ZsGreen antibodies.

We further tested the ZsGreen-positive and -negative sorted fractions by culturing sorted cells in vitro under conditions that allow expansion of myogenic progenitors (medium containing

serum, chick embryonic extract, and bFGF). ZsGreen$^+$ sorted cells plated on a gelatin-coated surface expanded as small round cells, which grew into three-dimensional colonies and sporadically fused to form multinucleated myotubes (Fig. 2A). On the other hand, cells from the negative fraction exhibited a fibroblastic morphology and grew strongly attached to the plastic (Fig. 2A). When medium was switched to promote differentiation, ZsGreen$^+$ sorted cells fused and formed large numbers of typical multinucleated myotubes and a residual population of undifferentiated cells, whereas negative-sorted cells did not form myotubes (Fig. 2A). The myogenic character of the ZsGreen$^+$ sorted fraction and lack thereof in the ZsGreen^{neg} fraction was supported by RT-PCR analyses of these cultures for specific myogenic genes (Fig. 2B). To further evaluate the myogenic potential of the Pax7-ZsGreen population, we established single-cell clones by sorting individual ZsGreen$^+$ cells directly from muscle digests into gelatin-coated 96-well dishes. All clones that arose (192 of 588 wells) had the morphology described above. On the other hand, under the same culture conditions, ZsGreen^{neg} cells were not able to expand from single cells (Fig. 2D). To evaluate the frequency of myogenic progenitors in the ZsGreen-negative fraction, we therefore plated increasing numbers of cells in each well and found that at 500 cells per well, approximately one-third of wells had growth after 8 days. We then analyzed individual cultures derived from single ZsGreen$^+$ cells or 500 ZsGreen^{neg} cells by immunostaining for Pax7, MyoD, or MyHC (Fig. 2C, 2D). All of the clones expanded from ZsGreen$^+$ cells contained a population of MyoD- and MyHC-positive cells, and 79% had some Pax7-positive cells (Fig. 2D). On the other hand, the majority of the cultures (90%) obtained from the negative cells were nonmyogenic, based on the absence of immunoreactivity for Pax7, MyoD, or MyHC (Fig. 2D). This means that although the negative fraction does have some myogenic progenitors, the positive fraction is approximately 5,000-fold enriched.

Surface Marker Profile of Pax7-ZsGreen$^+$ Cells In Vivo

Pax7-ZsGreen$^+$ cells from hind limb muscle and diaphragm of 3-month-old male and female mice were analyzed for expression of cell surface markers. ZsGreen$^+$ cells from both sources showed relatively similar expression patterns and were uniformly positive for CD29 and CD34 and negative for CD105, PDGFRα, c-Kit, and CD45 (Fig. 3). The markers CD8, CD 31, CD41, CD61, CD150, PDGFRβ, SSEA-1, SSEA-3, and SSEA-4 were also not expressed (not shown). Slightly more than half of the ZsGreen$^+$ cells isolated from total limb muscle digests were positive for CXCR4. A small fraction of cells gated positive for both M-cadherin and PSA-NCAM; however, they were at the edge of a negative population and most likely represent low-level nonspecific staining of these antibodies. The majority of cells were Sca1-negative, but a clear subpopulation expressed this marker at relatively high levels. These findings correlate with previous attempts to enrich satellite cells by positive selection for CD34 as well the combination of CD29 and CXCR4 [6, 10, 11]. Pax7$^+$ cells of the diaphragm were similar to those of the hind limb, with the exception of increased frequency of expression of CXCR4 and Sca1 (Fig. 3). None of these markers uniquely labeled Pax7$^+$ cells as all were expressed abundantly in the Pax7-ZsGreen^{neg} fraction (Fig. 3).

Age-Related Changes in Pax7-ZsGreen$^+$ Cell Frequency and Phenotype

To evaluate whether the nature or frequency of Pax7-ZsGreen$^+$ cells changed with age, we analyzed cells in pooled hind limb muscle digests of 1-week-old and 1-, 3-, 6-, and 12-month-old

mice (Fig. 3, 4A). To reduce the variation associated with enzymatic preparation, samples from each age group were processed simultaneously in each experiment ($n = 6$). We observed a clear age-related decline in satellite cell frequency, with neonates having approximately 4% of hind limb mononuclear cells expressing Pax7-ZsGreen, compared with less than 1% of cells in 1-year-old mice (Fig. 4A). We consistently noted that the expression level of Pax7-ZsGreen was higher in older mice, reflected in better separation of the labeled cell fraction (Fig. 4A, left panels). We also evaluated the frequency of satellite cells within different muscle types from hind limb, forelimb, trunk, head, and diaphragm of 1- and 6-month-old male littermates ($n = 3$). We found the highest frequencies of Pax7-ZsGreen$^+$ cells in the limb muscles, and aging clearly led to reductions in frequency in limb muscles (Fig. 4B). In each of TA, EDL, soleus, biceps, and triceps, the frequency of labeled mononuclear cells was greater than 1% in 1-month-old mice and less than 1% in 6-month-old mice (Fig. 4B). In other muscles, including diaphragm, the downward trend was not obvious between 1 and 6 months of age. It is important to note that decreasing frequency may not necessarily be due to decreasing absolute numbers but also to increasing numbers of nonexpressing cells from older mice. In addition, the percentage of positive cells may vary depending on the isolation conditions (i.e., digestion protocol).

When we analyzed the Pax7-ZsGreen$^+$ cells of pooled hind limb muscle digests from different age groups for surface antigen expression, we found that CD29 and CD34 remained uniformly expressed and that the frequency of CXCR4$^+$ cells did not change, but that Sca1 was expressed on a slightly larger fraction of cells as mice aged. The same analysis was performed in the diaphragm (not shown), with comparable results.

Injury-Associated Changes in the Pax7-ZsGreen$^+$ Cells In Vivo

To evaluate changes in the surface marker phenotype of the satellite cells during regeneration, we induced muscle injury with cardiotoxin. Seventy-two hours postinjection, we observed marked differences in the satellite cell phenotype. Pax7-ZsGreen$^+$ cells displayed increased forward and side scatter, indicating that they were much larger, as would be expected with activation from quiescence (Fig. 4C, left panels). In addition, they had dramatically altered their surface antigen expression profile. The frequency of cells expressing the satellite cell-specific markers, CD34, CD29, and CXCR4 was reduced, and a large subpopulation now expressed Sca1 (Fig. 4C, right panels).

In Vitro Expansion of Myogenic Progenitors from Pax7-ZsGreen$^+$ Sorted Cells

We sorted Pax7-ZsGreen-positive and -negative cells from hind limb muscle of 3-month-old male and female mice and expanded them in vitro on gelatin-coated dishes in proliferation medium for 2 weeks. Cultures derived from the ZsGreen$^+$ sorted cells retained CD29 (β1 integrin) expression, but the majority of cells lost expression of CD34 when cultured in vitro. They also expressed PSA-NCAM more uniformly and remained predominantly negative for PDGFRα, whereas cultures derived from the ZsGreen^{neg} sorted cells showed the opposite phenotype, becoming positive for PDGFRα and remaining mainly negative for PSA-NCAM (Fig. 5A). Approximately 15% of the ZsGreen$^+$ sorted cells continued to express Pax7 at low levels, indicated by weak ZsGreen fluorescence, after 2 weeks in culture, whereas the ZsGreen^{neg} sorted cells remained negative (Fig. 5A, far right panels). The same overall phenotype was observed for cells expanded from the diaphragm (Fig. 5A, lower
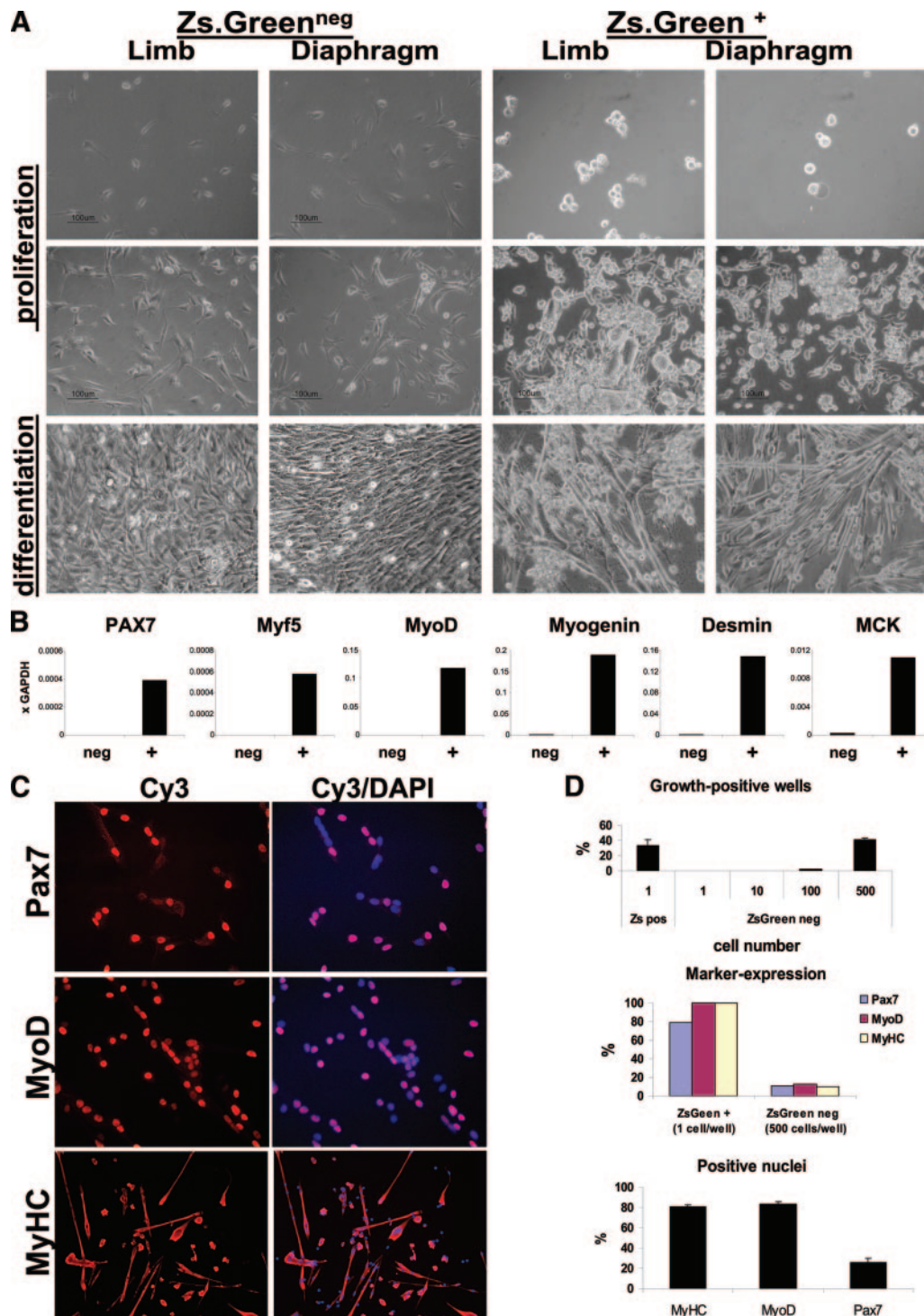
Figure 2. Direct isolation of satellite cells from Pax7-ZsGreen mice. **(A):** Morphology of ZsGreen+ and ZsGreen^neg sorted cells from limb and diaphragm of 3-month-old male and female mice, 3 (top row) and 9 (middle row) days after sorting and expansion in proliferation medium. Bottom row: Morphology of the expanded cells after 2 days in differentiation medium. Note that only ZsGreen+ cells differentiated into myotubes. **(B):** Real-time reverse transcription-polymerase chain reaction for myogenic genes in Pax7-Zsgreen+ (+) or Pax7-Zsgreen-neg sorted cells expanded in vitro for 7 days in proliferation medium. **(C):** Immunofluorescence for Pax7, MyoD, and MyHC (in red) in clones obtained from single ZsGreen+ cells. DAPI (blue) was used for counterstaining of the nuclei. Clones were expanded on gelatin-coated surfaces in myogenic proliferation medium for 8 days. **(D):** Quantification of the plating efficiency of ZsGreen+ and ZsGreen^neg sorted cells (top panel). Note that the ZsGreen^neg cells could not expand from single cells. All of the colonies obtained from the ZsGreen+ cells were myogenic based on the presence of Pax7-, MyoD- or MyHC-expressing cells within the clone (middle panel). The bottom panel represents the percentage of Pax7-, MyoD-, and MyHC-pos cells within each clone derived from ZsGreen+ cells. Abbreviations: DAPI, 4′,6-diamidino-2-phenylindole; GAPDH, glyceraldehyde-3-phosphate dehydrogenase; MyHC, myosin heavy chain; neg, negative; pos, positive.
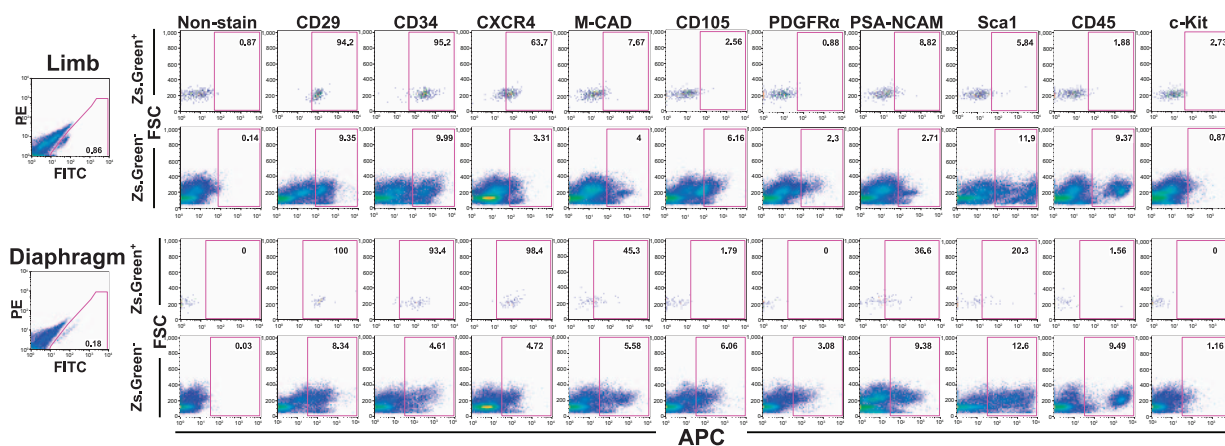
Figure 3. Surface marker profile of Pax7-ZsGreen$^{+/-}$ cells in limb and diaphragm. Fluorescence-activated cell sorting analyses for different surface markers on Pax7-ZsGreen$^+$ and -negative cells in hind limb and diaphragm in 3-month-old muscle. The *x*-axis shows the APC channel, and the *y*-axis shows FSC. Abbreviations: FITC, fluorescein isothiocyanate; FSC, forward scatter; M-CAD, M-cadherin; PDGFRα, platelet-derived growth factor receptor α.

series). Expanded ZsGreen$^+$ cells from the limb and diaphragm expressed MyoD and M-cadherin and sporadically differentiated into multinucleated cells expressing myosin heavy chain (Fig. 5C). We noted higher Pax3 expression in diaphragm-derived cultures (Fig. 5B). Accordingly, Pax3 is known to be expressed in the satellite cells of diaphragm but not in every limb muscle [6], although limb muscle satellite cells may transiently express Pax3 in vitro [29]. When induced to differentiate by growth factor withdrawal, expanded cells downregulated expression of Pax7, Myf5, and MyoD and increased expression of the terminal differentiation marker MCK (Fig. 5B). Notably, we observed that even in differentiation conditions some of the cells retained their round shape without undergoing differentiation (Fig. 2A). These cells could be washed off the plates, and when analyzed separately, they showed a myogenic transcription profile similar to undifferentiated cells growing in proliferation medium and were able to continue proliferating if transferred back to proliferation medium (data not shown).

Pax7-ZsGreen$^+$ Cells Can Be Expanded in Suspension

We observed that Pax7-ZsGreen$^+$ cells cultured in uncoated tissue culture plastic proliferated in suspension (Fig. 6A). This was most clearly evident 3 days after sorting, when large floating aggregates were present. By day 4, many aggregates attached to the plastic, and cells began spreading out (data not shown). The floating cells could be collected and replated, where they continued proliferating in suspension and spontaneously attached to the plastic. Likewise, the adherent fraction proliferated as a monolayer but also regenerated some floating cells. At day 14, we compared the phenotype of adherent cells to that of the floating cells and we found that most flow cytometric parameters were comparable, although adherent cells showed a greater fraction of both Sca1$^+$ and CD105$^+$ cells (Fig. 6B). Higher levels of Pax7, Pax3, Myf5, and MyoD were observed in the floating fraction (Fig. 6C).

Although preplating has been used as a means of enriching satellite cells [31], deliberate suspension culture of prospectively isolated satellite cells has not been reported. To rigorously address the myogenic potential of cells expanded in suspension culture, we initiated suspension cultures from sorted ZsGreen$^+$ cells from 1-month-old male mice, expanded them exclusively in suspension for 8 days (using low-adherence plastic and discarding any adherent fraction that formed), and injected the expanded cells (2,000 or 10,000 cells per injection) into cardio-

toxin-injured TA muscles of dystrophin-deficient (mdx$^{-/-}$) mice. Three weeks after transplantation we found that the expanded cells had engrafted and differentiated, as evidenced by clusters of 20–30 dystrophin$^+$ fibers in TA muscle (Fig. 6D). The number of dystrophin-positive fibers correlated with the dose of cells and was significantly higher than the background determined in the contralateral leg, injected only with PBS (Fig. 6E).

DISCUSSION

For the accurate study of particular cell types within complex tissues, cell-autonomous labeling with specific markers is essential. In the last decade significant progress has been made in understanding the surface marker profile of the satellite cell population (reviewed in [18, 32]). These studies are based on immunohistochemistry for antigens expressed in the cells positioned beneath the basal lamina, or flow cytometric sorting for cells expressing different surface antigens from total muscle digests followed by testing for myogenic properties. Two flow cytometry studies are particularly relevant here. The first showed that within the myofiber-associated mononuclear fraction, the CD45$^-$Mac-1$^-$CXCR4$^+$β1-integrin$^+$ population is highly enriched for myogenic progenitors [10]. The second used a Pax3-green fluorescent protein (GFP) reporter mouse and found that Pax3-expressing cells in diaphragm are small nongranular cells, positive for CD34 and negative for CD45 and Sca1 [6]. A limitation of the Pax3 reporter is that although Pax3 is associated with the satellite cells of the diaphragm, almost no quiescent satellite cells in the limbs express Pax3. However, by using the GFP$^+$ population of diaphragm as a reference to set forward and side scatter gates, it was possible to sort myogenic progenitors from limb muscles of these mice using only CD34 expression, and these sorted cells were able to restore dystrophin expression in mdx$^{-/-}$ mice [6]. Using the Pax7-ZsGreen reporter mice described here, we have been able to conclusively determine the surface marker phenotype of the Pax7$^+$ skeletal muscle stem cell. We show that these cells invariably express CD34 and CD29 (β1-integrin) regardless of muscle type or age. Prior to this study, it was unclear whether these markers identified all skeletal muscle stem cells or a subpopulation [9, 10]. Following injury, the frequency of Pax7$^+$ cells that express CD29, CXCR4, and CD34 decreases, and the frequency of cells expressing Sca-1 increases. This has obvious implications for
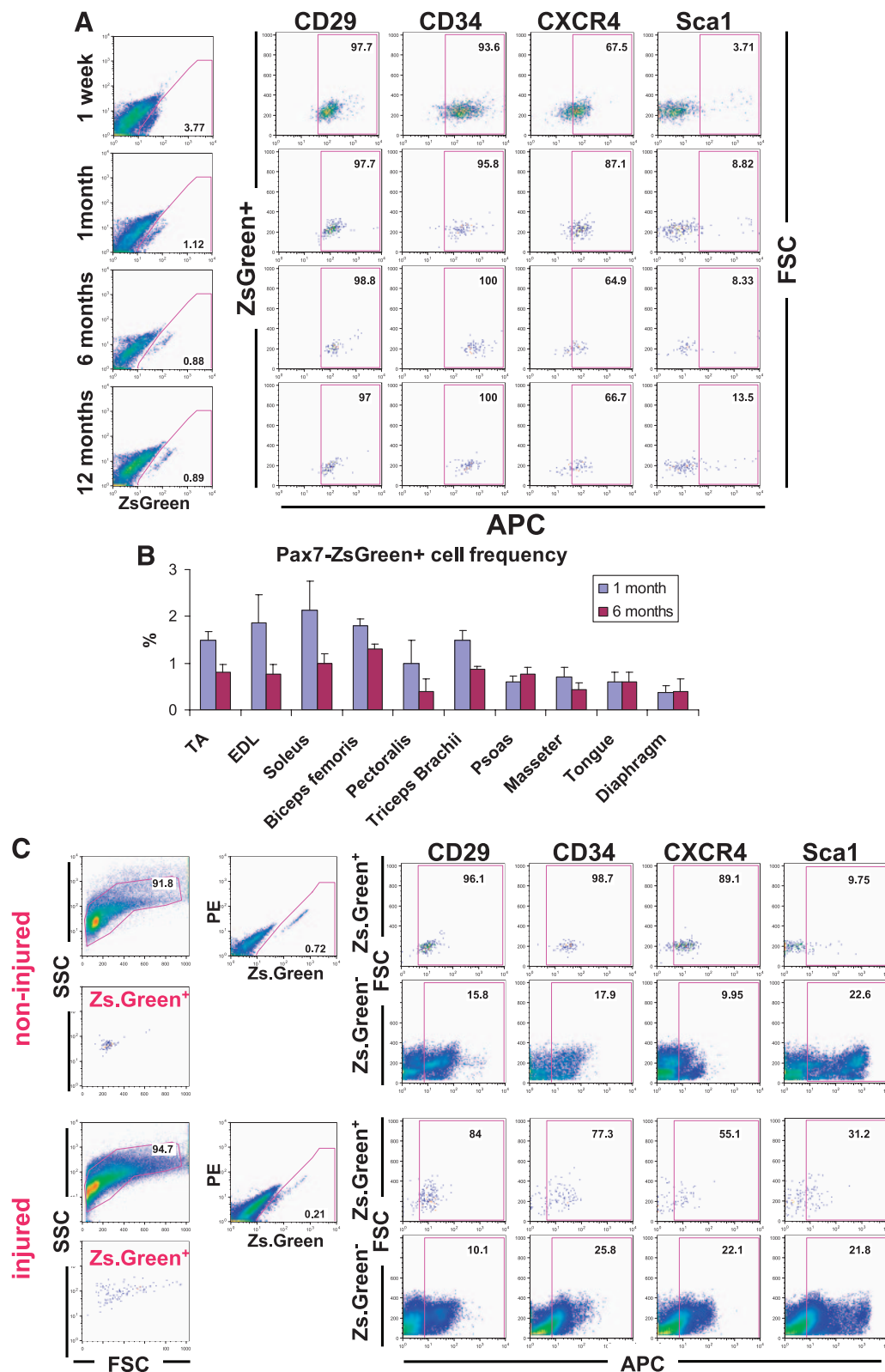
Figure 4. Age-, injury-, and muscle-type-dependent variation in Pax7-ZsGreen+ cells. **(A):** Surface marker profile of ZsGreen+ cells in 1-week-old and 1-, 6-, and 12-month-old mice. The left column shows green (x-axis) versus red (y-axis) fluorescence. Other columns show APC-conjugated antibody staining (x-axis) versus FSC (y-axis) of gated ZsGreen+ cells. The frequency of ZsGreen+ cells decreased with age, and surface marker profile remained constant, although Pax7 expression increased with age. **(B):** Frequency of labeled cells in different muscles of 1- and 6-month-old mice. **(C):** Surface marker profile of ZsGreen+ cells 3 days after injury. One hind limb of each Pax7-ZsGreen mouse was injured with multiple injections of cardiotoxin, and the other (noninjured) was used as a control. Three days after the injury, Pax7-ZsGreen+ cells from injured and noninjured legs were analyzed for expression of various surface markers. Abbreviations: FSC, forward scatter; SSC, side scatter; TA, tibialis anterior.
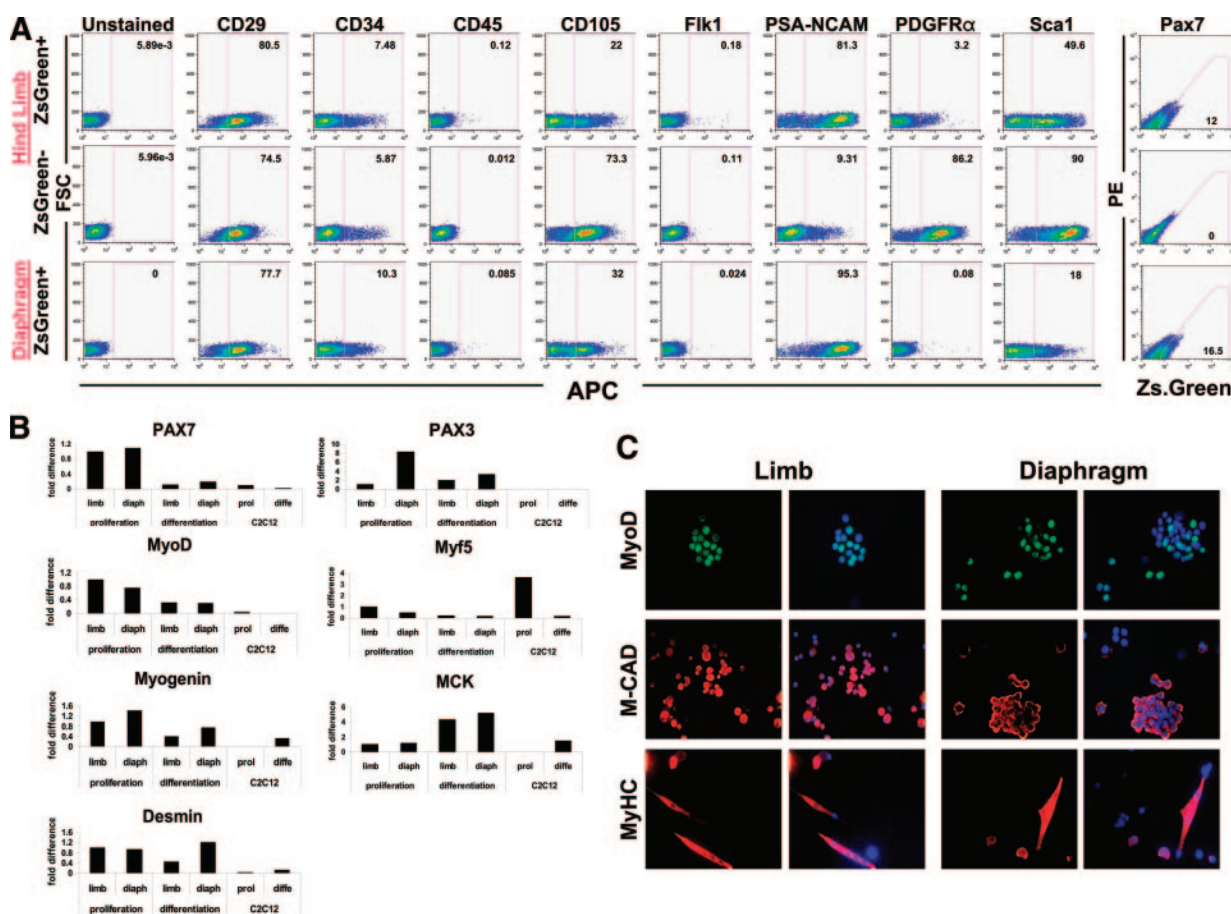
Figure 5. Characterization of Pax7-ZsGreen$^{+/-}$ cells expanded in vitro. **(A):** Surface marker profile of ZsGreen$^+$ and -negative cells from limb and diaphragm (diaph) expanded in vitro for 2 weeks. Staining of APC-conjugated antibodies is shown on the x-axis, and FSC is shown on the y-axis. The right column shows green (x-axis) versus red (y-axis) fluorescence. Note that some cells of the initial sorted ZsGreen$^+$ cells remained green in culture. **(B):** Real-time reverse transcription-polymerase chain reaction for expression of myogenic genes in expanded and differentiated cells from limb and diaphragm. Murine myoblast cell line-C2C12 in proliferation medium (prolif) or differentiation medium (diffe) was used as a control. **(C):** Immunofluorescence for MyoD, M-CAD, and MyHC in proliferating cells. 4′,6-Diamidino-2-phenylindole (blue) labeled the nucleus in the right-hand panel of each pair. Abbreviations: FSC, forward scatter; M-CAD, M-cadherin; MyHC, myosin heavy chain.

surface marker-based studies attempting to purify satellite cells following injury, and additional experiments carefully evaluating cell surface and transcriptional changes at multiple time points following injury are clearly warranted. The reporter mice that we have described will allow further exploration of satellite cell physiology, for example, whole genome expression analysis of satellite cells from different muscle groups, such as limb, head, or diaphragm, or from different mutant backgrounds.

We show that the frequency of Pax7$^+$ cells declines as mice age. Rapidly growing mice, such as those analyzed at 1 week of age, have a significantly elevated frequency of Pax7$^+$ cells, and many of these cells are very dim. This may be explained in part by the intensive muscle growth of young animals, resulting in a relative excess of myoblasts with perdurance of the ZsGreen protein. Histological studies based on the morphology, location, and immunostaining of satellite cells have also shown that satellite cell frequency decreases significantly with age. The dynamic of satellite cell decline has been reported to be different among different muscles; for example, depletion in EDL was observed in the first year of life, whereas in soleus it was most significant at age 2 [33]. Age-related declination in satellite cell frequency has been reported in rat [34, 35], mouse [36], and human [37]. By evaluating various muscles at 1 and 6 months of age, we found that the decline of Pax7-expressing cells was significant in all limb muscles but was not significant in most

muscles of the head and trunk, or in diaphragm, at the 6-month time point. Besides the reduction in frequency of Pax7-expressing cells, the principal age-related change is that Pax7 was expressed at higher levels in aged mice. The functional significance is presently unclear since we did not observe any differences in myogenic potential between satellite cells sorted from different age groups (data not shown). Using an in vitro culture system it has been shown that the myogenic potential of satellite cells does not decrease with the age [33] and that the regenerative potential of transplanted myoblasts correlates more strongly with age of the host than that of the donor [38].

We show that 3%–16% of Pax7-expressing cells are positive for Sca1. Sca1$^+$ cells are larger and more granular than the majority of satellite cells. A significant number of activated satellite cells acquire Sca1 expression after injury, as do the majority of Pax7-ZsGreen$^+$ sorted cells in culture. We also found that in mixed adherent/suspension cultures, the adherent myogenic progenitors expressed higher levels of Sca1 than did the floating cells. Remarkably, almost all of the ZsGreen^{neg} sorted cells following ex vivo culture expressed Sca1. Freshly sorted CD45$^-$CD34$^{+/-}$Sca1$^+$ cells from murine muscle were shown not to exhibit myogenic activity when differentiated in vitro [10]. These results suggest that Sca1 negativity is a useful parameter by which to gauge the myogenic regenerative potential of a given population. Besides Sca1, PDGFRα and CD105
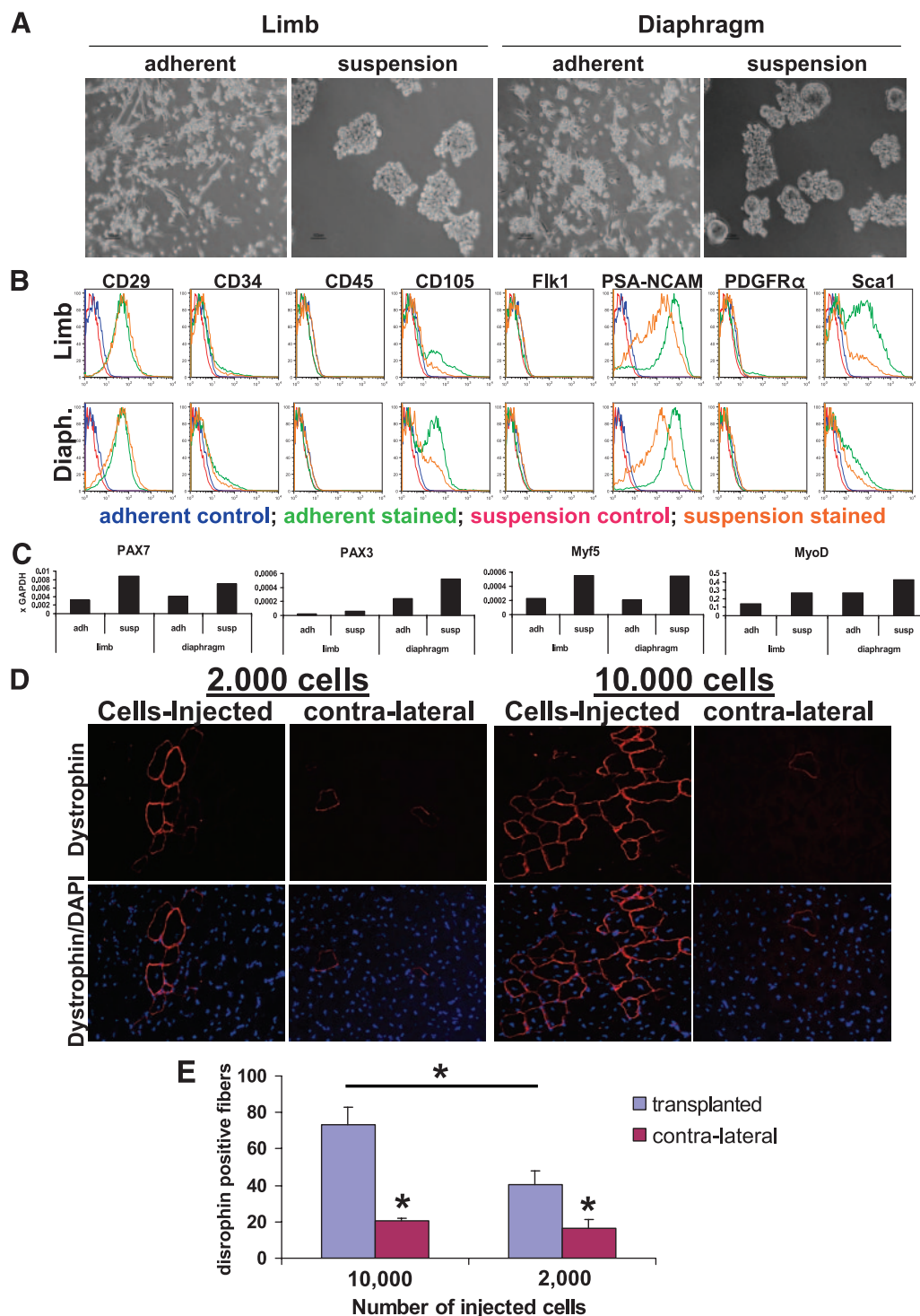
Figure 6. Muscle progenitors expand as adherent (adh) and floating cells in vitro and restore dystrophin expression in MDX mice. **(A):** Cell morphology of ZsGreen^{+} cells from limb and diaphragm (diaph). expanded in vitro. adh cells had a round to elongated shape. Cells that grew in suspension had a round shape and a tendency to grow in clumps. **(B):** Fluorescence-activated cell sorting analysis of cultures (susp and adh) initiated with ZsGreen^{+} cells. The blue trace indicates staining of adh cells; the red trace indicates staining of the susp. **(C):** Real-time reverse transcription-polymerase chain reaction analyses for myogenic regulators in susp and adh cultures of ZsGreen^{+} cells. **(D):** Immunofluorescence for dystrophin expression. ZsGreen^{+} cells were expanded in susp for 8 days, and 2,000 or 10,000 cells were transplanted into cardiotoxin-injured tibialis anterior muscle of mdx^{−/−} mice ($n = 4$). The cont-lateral leg was used as a control and was injected with phosphate-buffered saline. Three weeks post-transplantation, muscles were analyzed for dystrophin expression. Red represents dystrophin staining, and blue indicates DAPI staining of the nuclei. Note the presence of clusters of fibers expressing dystrophin in the transplanted leg, but only rare single revertant fibers in the contra-lateral leg. **(E):** Quantification of the dystrophin-positive fibers in cell-injected and contra-lateral legs. The results represent mean ± SE ($p < .01$). Abbreviations: DAPI, 4′,6-diamidino-2-phenylindole; GAPDH, glyceraldehyde-3-phosphate dehydrogenase; PDGFRα, platelet-derived growth factor receptor α.

also labeled cells expanded in vitro from the ZsGreen[neg] population. PDGFRα is particularly useful because it labels around 90% of cells expanded in vitro from the negative sorted fraction but only a small fraction of those from the ZsGreen[+] sorted fraction. An additional useful marker having the opposite pattern is PSA-NCAM, which labels almost all of the positive but not the negative cells. Mouse myogenic progenitors express NCAM and PSA-NCAM during proliferation and differentiation in vitro [39], and because in vivo PSA-NCAM was only transiently detected in developing fibers, it was proposed to be an early marker for muscle regeneration [40]. The almost exclusive distribution of PDGFRα on nonmyogenic cells and PSA-NCAM on myogenic cells and the biased expression of CD105 and Sca1 make these four markers useful for evaluation of myogenic purity of satellite cell ex vivo expansion cultures, whereas the markers that work best for prospective isolation (CD34 and CD29) are not useful in this regard. This is important because at present there is a dearth of markers for determining or enriching the myogenic purity of such cultures. CD56 (non-polysialation-specific NCAM1) is commonly used on human myoblasts [41, 42], and desmin staining (an intracellular antigen not useful for purifying cells from heterogeneous cultures) is used in mouse, as is the laborious method of differentiating, immunostaining, and quantifying cells expressing markers of differentiated muscle.

Various methods of establishing and maintaining relatively homogeneous myoblast cell cultures are in common use. One approach is to obtain single myofibers by collagenase digestion and repeated trituration of muscle tissue. The myofiber is then cultured in serum-rich medium on surfaces coated with laminin, collagen, gelatin, or Matrigel (BD Biosciences). Under these conditions, satellite cells activate and proliferate by spreading on the substrate [8, 29]. This isolation technique gives a relatively homogeneous population of myogenic cells, but it is laborious and time-consuming, making it difficult to obtain a sufficient quantity of progenitors at early passage to be used for transplantation. The other common method, preplating, separates cells on the basis of differential adherence [31, 43, 44]. Cells from enzymatically dissociated muscle are plated on collagen-coated flasks, and the fibroblastic cells are allowed to attach for a short period, after which the nonadherent cells are transferred to a new flask. When this procedure is repeated daily for 5 days, up to 95% of the cells express desmin [31]. Although preplating selects for nonadherent cells, studies have invariably been performed on the adherent fraction resulting from each preplating. We noticed that directly isolated ZsGreen^{+} satellite cells plated on collagen- or gelatin-coated flasks had a tendency to attach and then undergo several rounds of replication and present a high level of spontaneous differentiation. On the other hand, cells cultured on uncoated surfaces or on low-adherence plastic expanded without prominent differentiation. Analysis of both fractions, adherent and floating, demonstrated better myogenic purity and less differentiation in the nonadherent fraction. Remarkably, cells expanded in suspension demonstrated significant transplantation potential. Suspension culture in low-adherence dishes is also applicable for enrichment and expansion of myogenic progenitors from wild-type mice (unpublished observations).

CONCLUSION

Unlike the hematopoietic stem cells of bone marrow, muscle stem cells cannot be retrieved in great quantity without doing significant harm to the donor—muscle biopsies in humans are by necessity limited to small quantities of tissue. Prospective isolation by flow cytometry followed by suspension culture may offer the best approach for expanding muscle regenerating cells, if and when cell transplantation is tested for the treatment of muscular dystrophy.

ACKNOWLEDGMENTS

DISCLOSURE OF POTENTIAL CONFLICTS OF INTEREST

The authors indicate no potential conflicts of interest.

REFERENCES

1 Schultz E. Satellite cells in normal, regenerating and dystrophic muscle. Adv Exp Med Biol 1985;182:73–84.

2 Bischoff R. A satellite cell mitogen from crushed adult muscle. Dev Biol 1986;115:140–147.

3 Mauro A. Satellite cell of skeletal muscle fibers. J Biophys Biochem Cytol 1961;9:493–495.

4 Schultz E, Gibson MC, Champion T. Satellite cells are mitotically quiescent in mature mouse muscle: An EM and radioautographic study. J Exp Zool 1978;206:451–456.

5 Snow MH. A quantitative ultrastructural analysis of satellite cells in denervated fast and slow muscles of the mouse. Anat Rec 1983;207: 593–604.

6 Montarras D, Morgan J, Collins C et al. Direct isolation of satellite cells for skeletal muscle regeneration. Science 2005;309:2064–2067.

7 Collins CA, Olsen I, Zammit PS et al. Stem cell function, self-renewal, and behavioral heterogeneity of cells from the adult muscle satellite cell niche. Cell 2005;122:289–301.

8 Kuang S, Kuroda K, Le Grand F et al. Asymmetric self-renewal and commitment of satellite stem cells in muscle. Cell 2007;129:999–1010.

9 Beauchamp JR, Heslop L, Yu DS et al. Expression of CD34 and Myf5 defines the majority of quiescent adult skeletal muscle satellite cells. J Cell Biol 2000;151:1221–1234.

10 Sherwood RI, Christensen JL, Conboy IM et al. Isolation of adult mouse myogenic progenitors: Functional heterogeneity of cells within and engrafting skeletal muscle. Cell 2004;119:543–554.

11 Cerletti M, Jurga S, Witczak CA et al. Highly efficient, functional engraftment of skeletal muscle stem cells in dystrophic muscles. Cell 2008;134:37–47.

12 Cornelison DD, Filla MS, Stanley HM et al. Syndecan-3 and syndecan-4 specifically mark skeletal muscle satellite cells and are implicated in satellite cell maintenance and muscle regeneration. Dev Biol 2001;239: 79–94.

13 Irintchev A, Zeschnigk M, Starzinski-Powitz A et al. Expression pattern of M-cadherin in normal, denervated, and regenerating mouse muscles. Dev Dyn 1994;199:326–337.

14 Cornelison DD, Wold BJ. Single-cell analysis of regulatory gene expression in quiescent and activated mouse skeletal muscle satellite cells. Dev Biol 1997;191:270–283.

15 Wagers AJ, Conboy IM. Cellular and molecular signatures of muscle regeneration: Current concepts and controversies in adult myogenesis. Cell 2005;122:659–667.

16 Rantanen J, Hurme T, Lukka R et al. Satellite cell proliferation and the expression of myogenin and desmin in regenerating skeletal muscle: Evidence for two different populations of satellite cells. Lab Invest 1995;72:341–347.

17 Zammit PS, Golding JP, Nagata Y et al. Muscle satellite cells adopt divergent fates: A mechanism for self-renewal? J Cell Biol 2004;166: 347–357.

18 Péault B, Rudnicki M, Torrente Y et al. Stem and progenitor cells in

skeletal muscle development, maintenance, and therapy. Mol Ther 2007;
15:867–877.

19   Relaix F, Rocancourt D, Mansouri A et al. Divergent functions of murine Pax3 and Pax7 in limb muscle development. Genes Dev 2004;18:1088–1105.

20   Buckingham M, Relaix F. The role of pax genes in the development of tissues and organs: Pax3 and pax7 regulate muscle progenitor cell functions. Annu Rev Cell Dev Biol 2007;23:645–673.

21   Gros J, Manceau M, Thome V et al. A common somitic origin for embryonic muscle progenitors and satellite cells. Nature 2005;435:954–958.

22   Relaix F, Rocancourt D, Mansouri A et al. A Pax3/Pax7-dependent population of skeletal muscle progenitor cells. Nature 2005;435:948–953.

23   Seale P, Sabourin LA, Girgis-Gabardo A et al. Pax7 is required for the specification of myogenic satellite cells. Cell 2000;102:777–786.

24   Kuang S, Charge SB, Seale P et al. Distinct roles for Pax7 and Pax3 in adult regenerative myogenesis. J Cell Biol 2006;172:103–113.

25   Asakura A, Seale P, Girgis-Gabardo A et al. Myogenic specification of side population cells in skeletal muscle. J Cell Biol 2002;159:123–134.

26   Polesskaya A, Seale P, Rudnicki MA. Wnt signaling induces the myogenic specification of resident CD45+ adult stem cells during muscle regeneration. Cell 2003;113:841–852.

27   Dellavalle A, Sampaolesi M, Tonlorenzi R et al. Pericytes of human skeletal muscle are myogenic precursors distinct from satellite cells. Nat Cell Biol 2007;9:255–267.

28   Lee EC, Yu D, Martinez de Velasco J et al. A highly efficient Escherichia coli-based chromosome engineering system adapted for recombinogenic targeting and subcloning of BAC DNA. Genomics 2001;73:56–65.

29   Conboy IM, Rando TA. The regulation of Notch signaling controls satellite cell activation and cell fate determination in postnatal myogenesis. Dev Cell 2002;3:397–409.

30   Relaix F, Montarras D, Zaffran S et al. Pax3 and Pax7 have distinct and overlapping functions in adult muscle progenitor cells. J Cell Biol 2006;172:91–102.

31   Qu-Petersen Z, Deasy B, Jankowski R et al. Identification of a novel population of muscle stem cells in mice: Potential for muscle regeneration. J Cell Biol 2002;157:851–864.

32   Chargé SB, Rudnicki MA. Cellular and molecular regulation of muscle regeneration. Physiol Rev 2004;84:209–238.

33   Shefer G, Van de Mark DP, Richardson JB et al. Satellite-cell pool size does matter: Defining the myogenic potency of aging skeletal muscle. Dev Biol 2006;294:50–66.

34   Gibson MC, Schultz E. Age-related differences in absolute numbers of skeletal muscle satellite cells. Muscle Nerve 1983;6:574–580.

35   Nnodim JO. Satellite cell numbers in senile rat levator ani muscle. Mech Ageing Dev 2000;112:99–111.

36   Snow MH. The effects of aging on satellite cells in skeletal muscles of mice and rats. Cell Tissue Res 1977;185:399–408.

37   Kadi F, Charifi N, Denis C et al. Satellite cells and myonuclei in young and elderly women and men. Muscle Nerve 2004;29:120–127.

38   Carlson BM, Faulkner JA. Muscle transplantation between young and old rats: Age of host determines recovery. Am J Physiol 1989;256:C1262–C1266.

39   Dubois C, Figarella-Branger D, Pastoret C et al. Expression of NCAM and its polysialylated isoforms during mdx mouse muscle regeneration and in vitro myogenesis. Neuromuscul Disord 1994;4:171–182.

40   Figarella-Branger D, Nedelec J, Pellissier JF et al. Expression of various isoforms of neural cell adhesive molecules and their highly polysialylated counterparts in diseased human muscles. J Neurol Sci 1990;98:21–36.

41   Illa I, Leon-Monzon M, Dalakas MC. Regenerating and denervated human muscle fibers and satellite cells express neural cell adhesion molecule recognized by monoclonal antibodies to natural killer cells. Ann Neurol 1992;31:46–52.

42   Schubert W, Zimmermann K, Cramer M et al. Lymphocyte antigen Leu-19 as a molecular marker of regeneration in human skeletal muscle. Proc Natl Acad Sci U S A 1989;86:307–311.

43   Rando TA, Blau HM. Primary mouse myoblast purification, characterization, and transplantation for cell-mediated gene therapy. J Cell Biol 1994;125:1275–1287.

44   Qu Z, Balkir L, van Deutekom JC et al. Development of approaches to improve cell survival in myoblast transfer therapy. J Cell Biol 1998;142:1257–1267.

Prospective Isolation of Skeletal Muscle Stem Cells with a Pax7 Reporter

Darko Bosnakovski, Zhaohui Xu, Wei Li, Suwannee Thet, Ondine Cleaver, Rita C.R.
Perlingeiro and Michael Kyba

This information is current as of March 29, 2009

Updated Information & Services	including high-resolution figures, can be found at: http://www.StemCells.com/cgi/content/full/26/12/3194

ɑ AlphaMed Press